Article:
Akram, M. orcid.org/0000-0002-4427-4703, Milkowski, K. orcid.org/0000-0003-3122-8107, Gheit, A. et al. (4 more authors) (2026) Pilot-scale demonstration and practical challenges of bioenergy with CCS (BECCS) using rotating packed bed. Fuel, 405. 136562. p. 136562. ISSN: 0016-2361 (In Press)

https://doi.org/10.1016/j.fuel.2025.136562

Pilot-scale Demonstration and Practical Challenges of Bioenergy with CCS (BECCS) using Rotating Packed Bed

Muhammad Akram[a], Kris Milkowski[a], Abdulaziz Gheit[a], Janos Szuhanszki[a], Ihab Ahmed[a], Jon Lee[b], Mohamed Pourkashanian[a]

[a]Energy Innovation Centre (EIC), Department of Mechanical Engineering, University of Sheffield, Sheffield S10 2TN, UK

[b]School of Engineering, Newcastle University, Merz Court, Claremont Road, Newcastle upon Tyne NE1 7RU, UK

Corresponding author:

Muhammad Akram

m.akram@sheffield.ac.uk

Abstract

This paper presents findings of demonstration of CO_2 capture by rotating packed bed absorber using real biomass flue gases. There are two main objectives of the study presented here: (1) performance assessment of pilot scale rotating packed bed CO_2 capture absorber with real biomass flue gases (2) the impact of impurities in biomass flue gases on the solvent. The demonstration was carried out at the waste to energy and CO_2 capture facilities at the Energy Innovation Centre of the University of Sheffield. Rotating packed bed (RPB) absorber was used to capture CO_2 from biomass flue gas generated by a grate boiler. CO_2 loadings and solvent concentrations were measured using Mettler Toledo auto-titrator.

Particulates content of the flue gas was measured, and particulates were collected for further analysis at the boiler exit and absorber inlet by Electrical Low Pressure Impactor (ELPI®+) manufactured by Dekati®. The particulate samples were analysed by ICP-OES to investigate the impact of metals in the flue gas coming from the biomass on the solvent degradation. Solvent samples were collected and

analysed with ICP-MS and Ion Chromatography to quantify build-up of metals and anions in the solvent over time.

There is very limited information on this subject in open literature. The short-term tests presented here can serve as a starting point for further longer-term investigations into the impact of biomass flue gas contaminants on the solvent behaviour and the solvent management requirements during CO_2 capture from biomass flue gases.

Nomenclature

BECCS	Bio-Energy with CCS
CAPEX	Capital Expenditure
CCS	Carbon Capture and Sequestration
CV	Calorific Value
DETA	diethylenetriamine
EIC	Energy Innovation Centre
ELPI	Electrostatic Low Pressure Impactor
ESP	Electro-Static precipitator
EU	European Union
FTIR	Fourier Transform Infra-red spectrometry
HEA	N-(2-hydroxyethyl)-acetamide
HEF	N-(2-hydroxyethyl) formamide
IC	Ion Chromatography
ICP	Inductively Coupled Plasma
ICP-MS	Inductively coupled plasma – Mass Spectrometry
ICP-OES	Inductively Coupled Plasma – Optical Emission Spectroscopy
LCOE	Levelized Cost of Electricity
MCPD	Medium Combustion Plant Directive
MEA	Monoethanolamine
OPEX	Operational Expenses
PB	Packed Bed
PCCC	Post Combustion CO_2 Capture
PHW	Pressurised Hot Water
ppm	parts per million
RPB	Rotating Packed Bed

1 Introduction

Negative greenhouse gas emissions are required to achieve net zero targets to compensate for hard to abate industries such as steel, cement, and long-distance transport like shipping and aviation [1]. Arguably, negative emissions can be achieved either by direct air capture (DAC) or bioenergy with CCS (BECCS). DAC systems are normally small scale and can be installed anywhere to remove CO_2 from atmosphere. However, CO_2 capture plants for BECCS plants can only be installed next to a bioenergy plant. However, energy consumption per ton of CO_2 captured for DAC systems is currently higher as compared BECCS.

UK's biggest renewable power producer, Drax power station in North Yorkshire, providing 12% (14 TWh) of UK's renewable power using biomass (bio-energy) had reduced carbon emissions from the power plant by 80% [2] by switching from coal to biomass. Currently, four boilers at the Drax power plant are using biomass to generate 2.6 GW of renewable power. Decarbonizing the bio-energy i.e. deploying CO_2 capture at the biomass power plants such as Drax have huge potential for net negative emissions and to meet 2050 net zero targets set by the UK Government.

Solvent based post combustion CO_2 capture (PCCC) is the most advanced and well understood process and is a leading contender to be deployed to capture and store CO_2 from biomass flue gases and thus achieving negative CO_2 emissions.

Traditionally PCCC process employs packed columns for absorption and desorption. However, due to the slow rate of reaction of traditional CO_2 capture solvents such as Monoethanolamine (MEA), usually 30wt% solution, the size of the packed towers can be substantial in terms of height and diameter resulting in high CAPEX, OPEX and impact on LCOE. For example, a capture plant integrated with a 960MW coal fired power plant will require absorber and desorber sizes of approximately 20m x 64m and 13m x 40m, in diameter and height, respectively [3]. Rotating packed bed (RPB) initially proposed for CO_2 capture by Ramshaw and Mallinson [4] offers a next generation process intensified technology to address this challenge. RPBs enhance the mass transfer coefficient [5] by providing centrifugal force to improve slip velocity, flooding characteristics and interfacial shear stress.

Due to enhanced mass transfer coefficient, higher concentrations of solvent can be utilised in RPB absorbers as compared to conventional absorbers resulting in increase in capture capacity and thus reduction in costs of CO2 capture. The scale up of RPBs to industrial scale units could be a challenge. Maximum practical achievable diameter and speed of rotation will dictate the capture capacity. Moreover, wettability of packing and optimum L/G ratios to avoid flooding and channelling could also be decisive parameters for the scaleup. However, it is sometimes beneficial to install relatively smaller absorber units in parallel, particularly in the case of gas fired power plants which go frequent load changes to accommodate renewables intermittency. In this case some of the capture units can be turned on and off based on the load on the parent plant.

However, most of the studies so far on CO2 capture by RPBs has been conducted on lab scale [6-13]. Chamchan et al. 2017 [11] conducted a comparative study on PB and RPB absorber using 30% CO_2 content flue gas to represent blast furnace. Using 30 wt% MEA solvent it was demonstrated that the two types of absorbers performed similarly but the RPB has a volume of approximately one-third that of PB absorber. The RPB absorber had an inner diameter of 0.12 m, an outer diameter 0.36 m, and a height of 0.06 m. However, the PB absorber they used was very small (0.1m dia and 2m high) compared to conventional absorbers thus providing very short residence time for absorption. Moreover, the reboiler duties of ~8 GJ/ton of CO_2 obtained with both PB and RPB absorbers were almost double the optimum values.

Wu et al. 2017 [12] compared CO_2 capture performance using RPB and PB absorbers for gas turbine flue gas compositions using 7m (30 wt%) MEA and observed that with similar volume of packing, RPB absorber can capture 1.2 to 4.6 times higher amount of CO_2 depending upon the gas flow. Moreover, they observed that RPB performed better than PB even at higher lean loadings of 0.34 mol/mol indicating faster reaction rate with RPB even with shorter residence time. However, the RPB absorber used for the study was relatively small having the inner diameter of 2.5 cm, outer diameter 12.5 cm, and height of the packing of 2.3 cm.

Sheng et al. 2018 [13] investigated performance of PRB absorber under varying operational conditions using diethylenetriamine (DETA) solvent. The RPB they used had outer and inner diameters of 15cm and 5 cm, respectively and axial depth of packing of 5.3 cm. However, the study was focussed only on absorption rather than a cyclic absorption and desorption process as would be in the real plant.

Although some studies are performed on RPB at small scale, see Akram et al. 2025 [14] for further details, there is no open access practical demonstration of BECCS with RPB at pilot scale available in open literature. This project demonstrated the performance of a 1 tpd CO_2 capture capacity RPB absorber with real biomass flue gases generated by a 250 kW_{th} biomass boiler.

The particulates in biomass flue gas can carry volatile metals. Industrial biomass boilers are usually equipped with gas clean up technologies such as ESP and bag filters which can remove up to 99.9% particulates. However, there is still a chance that very fine sub-micron particle can pass through to the capture plant and accumulate over time. In this case, some of the volatile metals carried over with the particulates and enter the solvent can have impact on the capture process through solvent degradation and foaming resulting in increased operational costs. Moreover, they can shorten the plant lifetime through corrosion caused by the degradation products. Corrosion is caused mainly by degradation compounds such as Heat Stable Salts (HSS) [15-16]. Mechanisms of solvent degradation reactions are complex and are influenced by the presence of metals [17]. Therefore, during this study particulates emissions were monitored by a Dekati® ELPI®+ at the boiler exit and the absorber inlet. Particulate samples were also collected at both locations for post analysis by Inductively Coupled Plasma – Optical Emission Spectroscopy (ICP-OES). Moreover, solvent samples were collected from the plant frequently and analysed by ICP-OES and Ion Chromatography (IC) for build-up of metals and anions in the solvent, respectively.

2 Experimental facilities

Flue gas generated by biomass boiler was fed to the RPB absorber for CO_2 capture. Overall setup used for the demonstration experiments is provided as simplified flow diagram in Figure 1a. The Figure shows the schematic of the integrated biomass boiler and RPB CO_2 capture plant with an indication of particulates and gas sampling locations. Figure 1b shows picture of the RPB absorber and desorber installation.

MEA (35%wt) was used as solvent. Higher concentrations of MEA are expected to increase corrosiveness of the solvent. So, the 35wt% MEA is expected to be slightly corrosive and higher degradation potential than 30% MEA (considered as standard benchmark solvent for comparison with new more advanced solvents). However, on the other hand higher MEA concentrations have higher absorption capacity and thus can potentially reduce power consumption in the CO_2 capture process.

The rich and lean solvent samples were analysed by a Mettler Toledo auto-titrator for CO_2 loadings and MEA concentrations for all the test conditions. Moreover, biomass fuel was analysed and particulate samples at the boiler exit and absorber inlet were collected and analysed. Solvent samples were also collected and analysed using ICP and IC. Further details of the experimental setup and analytical measurements are provided in the following sections.

Figure 1: Overall experimental setup

2.1 Description of the capture plant

The pilot scale Rotating Packed Bed (RPB) CO_2 capture plant at the EIC is capable of capturing 1 tpd CO_2 based on 90% capture from coal combustion flue gas (~15% CO_2). The RPB has an inner diameter (D_i) of 95mm, an outer diameter (D_o) of 1100mm and an axial depth of 45 mm. Surface area of the packing is 1150 m^2/m^3 and void fraction is 0.914.

The RPB plant is integrated with the conventional packed bed (PB) plant. Both plants have full absorption and desorption cycles. Rotational speed on RPB absorber and desorber can go up to 800

174 rpm and 590 rpm, respectively. The operation can be switched between the two plants (RPB and PB
175 plants) by adjusting relevant valve positions. RPB desorber is fed with steam from a dedicated boiler
176 capable of delivering steam at up to 10 bar. The conventional packed bed stripper/reboiler is fed with
177 Pressurised Hot Water (PHW) and can be operated at up to 180 ^{o}C. Further details of the plant can be
178 found in Akram et al. 2025 [14]. For these tests, the RPB absorber was operated with the conventional
179 desorber to investigate RPB absorber performance for capture efficiency.
180 The capture plant is integrated with site combustion facilities including grate boiler/waste to energy
181 plant, gasifier, biodiesel engine and gas turbine. The plant can also be fed from a dedicated synthetic
182 gas mixing skid comprising 3 bulk gas streams: CO_2, N_2 and Air, each of 6-300 Nm^3/h flow range and a
183 trace gas (NO_2, SO_2) injection capability. During these tests flue gas generated by the grate boiler using
184 virgin wood was fed to the CO_2 capture plant, drawn via a fan located on the capture plant (inlet of the
185 absorber).
186 The capture plant is also equipped with gas clean-up/conditioning facilities for flue gas cleaning e.g.
187 Sulfur & HCl scrubbing. These steps can be applied to any flue gas source within the site. However, as
188 the gas analysis confirmed that there was not significant presence of SO_2 and HCl in the flue gas (~ 1
189 ppm), these treatment units were bypassed during these tests. This is in line with industrial application,
190 e.g. Drax, where the flue gas desulphurisation units were decommissioned after the switch from coal
191 to biomass fuels were completed. The flue gas was cooled down to near ambient temperatures before
192 entering the absorber due to long pipe run between the boiler and the capture plant. The gas entering
193 the absorber was considered saturated at ambient conditions while leaving the absorber was at higher
194 temperatures due to exothermic reaction between MEA and CO_2. As a result, net water loss can be
195 expected from solvent system. The flue gas path leaving the absorbers has two U-bends to remove
196 condensed water from the gas. The condensed water is directed back to the absorber sump. The
197 remaining water loss is compensated by transfer of water from water wash to the solvent system. This
198 water transfer is automatically controlled by maintaining liquid levels in the plant by the PLC control
199 system.

Flow rate of the flue gas into the absorber was measured by a pitot type flow meter. Gas analysis can be performed at 6 different locations in the plant. During these tests, gas analyses were carried out at the RPB absorber inlet and outlet. Alongside gas composition measurements, temperature and pressure were also recorded at both locations for mass balance calculations.

2.2 Description of the boiler

The 250 kWth moving grate fired biomass/WtE boiler, is capable of burning a range of virgin biomass and waste fuels. Further details of the biomass boiler are provided in Norizam et al. 2024 [18].

High combustion temperatures (1000-1100 ^{o}C) as well as appropriate residence time of the combustion gases ensure a clean burning process. Furthermore, particulate removal is achieved in two distinct steps using a multi cyclone system followed by an electrostatic precipitator (ESP) to adhere to the strict emissions limits of the Medium Combustion Plant Directive (MCPD). The directive applies emission limits values of SO_2 (200 mg/Nm^3), NO_x 650 (mg/Nm^3) and dust (50 mg/Nm^3) to units firing solid biomass with a rated thermal input of each unit equal to or greater than 1MW$_{th}$ and less than or equal to 5MW$_{th}$.

During these tests, gas analyses were only performed at the capture plant, RPB inlet and outlet. On the boiler side, exhaust gas oxygen content and combustion chamber temperatures were monitored to control the fuel and air flows to achieve the target CO_2 concentration in the flue gas.

2.3 Fuel:

Virgin wood chips were used as a fuel and thus a source of flue gas for the capture plant. The fuel was provided by a local Yorkshire based company, Maxchips. Table 1 shows analysis of the biomass alongside techniques used to perform them. Due to budget limitation only one biomass sample was analysed. However, the biomass for the whole test campaign was delivered as one load so it is not expected to have significant compositional differences.

Metal content of the biomass was of particular interest as some of the metals are found to have negative impact on MEA, benchmark solvent for this application. Therefore, biomass samples were analysed for several common metals found in biomass. For the analysis, the biomass samples were ashed, the ash was then digested with the aqua regia method. The resulting solution was filtered, diluted and run on the ICP-OES. Following standard methods were used for the analysis.

- ISO 16967:2015 Solid biofuels for the determination of major elements — Al, Ca, Fe, Mg, P, K, Si, Na and Ti
- ISO 16968:2015 Solid biofuels for the determination of minor elements

Table 1: Fuel analysis

Analysis	Units	Technique	As Received (AR) results	Dry Ground (DG) results
Gross CV	MJ/kg	Bomb calorimetry	14.4	19.18
Net CV	MJ/kg	By calculation	12.83	17.92
Moisture	%	Gravimetric	25	-
Ash	% w/w		0.4	0.5
Carbon	% w/w	Elemental analyser	37.2	49.6
Hydrogen	% w/w		4.3	5.8
Nitrogen	% w/w		0.4	0.5
Oxygen	% w/w	By calculation	32.7	43.5
Volatile matter	% w/w	Gravimetric	62.4	83.1
Fixed carbon	% w/w	By calculation	12.3	16.4
Sulphur/Sulphate	% w/w	Ion Chromatography	0.02	0.03
Chlorine/Chloride	% w/w		0.03	0.04

Antimony - Sb	mg/kg	ICP-OES	1.1	1.4
Chromium - Cr	mg/kg		3	4
Copper - Cu	mg/kg		2.9	3.8
Lead - Pb	mg/kg		0.9	1.2
Manganese	mg/kg		45	60
Nickel - Ni	mg/kg		2	2.6
Vanadium - V	mg/kg		0.3	0.4
Zinc - Zn	mg/kg		9.1	12
Aluminium - Al	mg/kg		97	129
Barium - Ba	mg/kg		10	14
Boron - B	mg/kg		1.7	2.3
Calcium - Ca	mg/kg		916	1220
Iron - Fe	mg/kg		100	133
Magnesium - Mg	mg/kg		125	166
Phosphorous - P	mg/kg		81	108
Potassium - K	mg/kg		378	504
Silicon - Si	mg/kg		50	67
Sodium - Na	mg/kg		94	125
Strontium - Sr	mg/kg		4.4	5.8
Titanium - Ti	mg/kg		5.7	7.6

2.4 Measurements:

Following measurements were recorded during the tests.

- Temperatures, flows and pressures on the CO_2 capture plant
- Gas concentrations and temperatures on the grate boiler

- Gaseous compositions were measured by Gasmet FTIR and a stack analyser
- Particulates were measured at the boiler exit and absorber inlet using Dekati® ELPI®+
- Particulate samples were collected with the Dekati® ELPI®+ and analysed by ICP-OES
- Acid-base titrations were performed for monitoring MEA concentration and CO_2 loadings
- Solvent samples were collected for post analysis by ICP-OES and IC

2.4.1 Gasmet DX4000 FTIR:

The gas samples from the plant are routed to the gas analysis setup (FTIR) through heated filters, heated sampling lines and a heated cabinet housing solenoids for sample switching. The sequence and sampling time is user defined and can be changed in the FTIR software as and when required. The entire sampling system is heated up to 180^{o}C to avoid condensation.

Two FTIRs were employed to continuously measure gas compositions at absorber inlet and outlet. As FTIR measurements are affected by unknown degradation products, a stack analyser (Servomax 4000 series with CO_2 sensor) was also used to measure CO_2 concentrations at the absorber outlet in parallel to the FTIR. The stack analyser measured dry gas so a chiller was used to remove water from the flue gas. The stack analyser was calibrated with certified gas compositions in cylinders provided by BOC.

2.4.2 Mettler Toledo auto-titrator:

To maintain the solvent composition and assess capture performance, solvent analyses were performed by Mettler Toledo auto-titrator to measure MEA concentration and CO_2 loadings in both the rich and lean solvent streams. For these tests, rich and lean solvent samples were collected directly from the plant and analysed manually using the titrator for MEA concentration and CO_2 loadings.

2.4.3 Dekati® ELPI®+:

The Dekati® ELPI®+ (Electrical Low Pressure Impactor), is a widely-used and well-characterized particle size spectrometer for real-time particle measurements. The ELPI®+ enables measurement of real-time particle size distribution and concentration in the size range of 6 nm – 10 µm at 10 Hz sampling rate. In the ELPI®+, particles are classified into 14 size fractions in a cascade impactor.

For these tests, the ELPI® analyser was used to monitor particulate concentrations and to collect particulate samples at the boiler exit and RPB absorber inlet. Polycarbonate impactor collection foils, coated with a high temperature grease (Apiezon-H), were used during the tests.

The PM sampling consisted of a PM10 cyclone, a Dekati ediluter, a Dekati low pressure impactor (ELPI+), a pressure gauge, and a vacuum pump. The flue gas was drawn using a stainless-steel probe with a diameter of 10 mm at a flowrate of 10 L/ min. The PM10 cyclone removed particles larger than 10µm aerodynamic diameter. An ejection diluter (Dekati®eDiluterTM) was used to dilute the sample with total dilution ratio (DR) of 25. Number and mass concentrations of particles were assessed based on discrete size distributions through the 14 stages (with size ranges of 10 nm – 10 µm) of the impactor. The whole sampling system including the sampling probe, cyclone, ELPI+, and the connecting tubes were all heated to a temperature of 180 ^{o}C to prevent the condensation of acidic gases and agglomeration of wet particles.

2.4.4 ICP

The particulates collected by ELPI®+ were digested in an acid prior to analysing by ICP. Digestion of sample was done by an open top method (for major metals 0.1ppm to % levels) for ICP analysis. The sample preparation procedure involved:

- Weigh the filter before placing into a clean dry 50ml conical flask
- Add 5ml of aqua regia and place the flask on a heating equipment
- Adjust the temperature so the acid just bubbles and brown fumes appear
- Digest the sample for 30 min, cool for 10min then remove the filter
- Make up to 50 ml in a volumetric flask with distilled water

2.4.5 Ion Chromatography

Ion Chromatography was used to measure anion concentrations in the solvent samples for acetate, formate, nitrate, nitrite and oxalate. Following methods were used for the analyses.

Instrument: ThermoScientific ICS5000; Column: AS19+AG19 4µm (2X250 2X50)

Temperature: 40 ^{o}C; Injection: 10µl

290 Method for oxalate: 0.25ml/min flow, 30min run, Eluent Isocratic: KOH, 15mM

291 Method for other anions: 0.25ml/min flow, 40min run, Eluent gradient: KOH, 2 to 30mM

292 3 Test matrix:

293 The experimental conditions used for the tests: Flue gas flow = 150 m^3/h; stripper pressure = 1.5 bara;
294 RPB absorber speed = 400 rpm. Solvent flow rate was changed to vary L/G ratio. The PHW temperature
295 was changed to achieve desired capture efficiency.
296 Table 2 presents average values of the measured parameters and their standard deviations, over 30 -
297 60 mins steady state test period. Each test took 6-8 hrs, resulting in 5-10 solvent circulations depending
298 upon the solvent flow. Absorber exit CO_2 concentration was monitored continuously. Flat line through
299 CO_2 concentration over a period (minimum 30 min.) was considered as a steady state.
300 Table 2: Test conditions (the values in the parentheses represent standard deviations

Flue gas conditions at absorber inlet					
Flow rate	CO_2 conc.	O_2 conc.	Temperature	Solvent flow	L/G ratio
m^3/h	%	%	°C	kg/h	kg/kg
149.86 (3.15)	10.59 (0.49)	10.68 (0.59)	9.0 (0.3)	352.97 (1.4)	1.8
149.98 (3.43)	10.84 (0.31)	10.74 (0.49)	14.2 (0.12)	386.1 (2.98)	2.0
150.04 (3.45)	10.55 (0.49)	11.11 (0.59)	14.2 (0.06)	428 (2.09)	2.2
150.04 (1.18)	10.41 (0.27)	11.41 (0.43)	13.8 (0.25)	470 (2.28)	2.4
149.97 (1.22)	10.56 (0.27)	11.63 (0.34)	14.4 (0.28)	511.9 (1.6)	2.6
150.0 (1.16)	10.29 (0.33)	11.89 (0.4)	9.3 (0.07)	699.9 (1.87)	3.0

301

302 4 Results and discussion:

303 Performance of the RPB absorber is assessed under varying L/G ratios. Moreover, potential
304 challenges faced by CO_2 capture from real biomass flue gases are highlighted in the following
305 sections.

4.1 Capture performance

Capture performance is normally measured as percentage removal of CO_2 (capture efficiency, %) and energy required to remove a unit amount of CO_2 (reboiler duty, GJ/ton of CO_2 removed). Moreover, capture performance is optimised based on these two performance indicators to achieve maximum capture efficiency at minimum reboiler duty. CO_2 loadings of rich and lean solvent streams are used to measure absorption and desorption capacity. Capture process can be optimised for minimum reboiler duty based on stripper temperature profiles. Results for the above-mentioned performance indicators are presented in the following sections. Comparative results of the RPB absorber with conventional packed bed absorber have been published in [14].

4.1.1 Capture efficiency and reboiler duty

Capture efficiency is calculated based on the CO_2 concentration at the inlet and outlet of the absorber. Figure 2 provides the results of reboiler duty and capture efficiency as a function of liquid to gas (L/G) ratio. Capture efficiency for all the tests was slightly lower than 90%, as it was hard to achieve steady state due to variations in the flue gas composition (see section 4.2.1). However, reboiler duty shown a variable trend ranging from 4.3 to 9.4 MJ/kg. At L/G ratio of 1.8, reboiler duty increased exponentially compared to that at L/G ratio of 2 indicating solvent flow was too low for the experimental conditions and significantly lower lean loading was required to achieve the desired capture efficiency. It can be observed from the figure that optimum reboiler duty of 4.3 MJ/kg is achieved at L/G of ~2. Beyond this L/G ratio, reboiler duty has slightly increasing trend with increase in L/G ratio.

The RPB absorber is driven by 4.7 KW motor. For these tests the RPB was operated at 400 rpm which is 50% of the full speed. The power consumption by the motor was not directly measured but can be roughly estimated by calculations. The calculated electricity usage by the motor at 50% of the rated capacity is 0.6 kW (2.2 MJ/h). This increases energy consumption (reboiler duty + motor consumption) by less than 2% for all the conditions tested.

Figure 2: Capture efficiency and reboiler duty as a function of L/G ratio

4.1.2 CO_2 loadings

Figure 3 shows CO_2 loadings as a function of L/G ratio. As can be observed from the figure that lean loading at L/G ratio of 1.8 is significantly lower than that at L/G ratio of 2 and the gap between the lean and rich loading at this L/G ratio is wider (higher solvent capacity requirement). This is an indication that stripper must work harder to achieve a desired capture efficiency under these conditions hence significantly higher reboiler duty as observed in Figure 2. Also, it can be noted that at L/G > 2, rich loading has slightly decreasing trend with increase in L/G ratio due to higher solvent flows. It is also worth noting that rich loading was always well below the theoretical maximum of 0.5 mol/mol for MEA indicating that solvent was not fully loaded. It could be due to low residence time in the RPB absorber. This also highlights that reboiler duty can be reduced by increasing residence time and thus increasing rich loading to close to theoretical maximum of 0.5 mol/mol and capture more CO_2. This subject is discussed in detail in Akram et al. [14] and RPB design improvements are proposed to improve capture efficiency and in turn reboiler duty.

Figure 3: CO_2 loadings as a function of L/G ratio

4.1.3 Stripper temperature profile

Temperature profile in the stripper is measured by nine thermocouples placed at different locations along the stripper height. Stripper temperature profiles can be characterised into three distinct modes; baseline region, inflection point and exponential region. Further details about these profile categories can be found in [19,20].

Figure 4 shows stripper temperature profile for the experiments. The second temperature measurement from the top of the column (at 7.1m height) is influenced by the incoming condensate from the reflux drum and thus is not included in the plot. It can be observed from the figure that at the lowest solvent flow rate tested, 353 kg/h (L/G = 1.8), stripper temperature profile lies in the exponential region. In order to achieve high capture efficiency under these conditions very low lean loading is required as shown in figure 3 resulting in high reboiler duty as shown in Figure 2. As the solvent flow rate increased, the temperature profile changed to transition region which is the desired

operational regime. As solvent flow is further increased, the temperature profile shifts to the left. As previously described, the lowest reboiler duty is measured at 386 kg/h solvent flow (L/G = 2). Temperature profile for this test is significantly different to that at L/G = 1.8 and lies in the transition region. The temperature profile for the L/G ratios of 2.2 – 2.6 is similar. With further increase in solvent flow, the profile slowly shifts to the left and eventually will fall into the baseline region with further increase in solvent flow.

Figure 4: Stripper temperature profile

The data presented highlights optimum operating regime under these conditions using the RPB. Based on the data obtained, the RPB absorber is now being upgraded to increase the packed volume to try to increase rich loading to maximum achievable with MEA (0.5 mol/mol). This may result in lowering reboiler duty.

4.2 Challenges

One of the major challenges during the test campaign was the flue gas composition variability leading to longer test times required for the capture plant to get to steady state. Moreover, carry over of volatile metals present in the biomass via particulates in the flue gas can influence the capture plant performance. These aspects are discussed in the following sections.

4.2.1 Flue gas composition variation

As mentioned previously, flue gas composition from the boiler to the capture plant was variable, resulting in longer test times for the capture plant to reach steady state. Figure 5 plots flue gas composition (O_2, CO_2, NO, CO) for a typical operational day at the inlet of the capture plant. As can be observed from the plot, CO_2 concentration varied from 8.7 to 11.4%. This is in conjunction with O_2 variation from 9.7 to 12.9% as shown in the plot. The O_2 concentration can vary due to several factors, including variable size or moisture content of the fuel, agglomeration or build-up of material on the boiler grate. Also, it is clear from the plot that when O2 level drops, a peak is observed in the CO concentration which was mostly around 800 ppm but occasionally reached ~1500 ppm. However,

382 average CO concentration over the day was ~70 ppm. CO_2, O_2 and NO content of the flue gas during
383 the day averaged at 10.29%, 11.5 % and 60 ppm, respectively. Both NO and NO_2 concentrations were
384 measured but NO_2 concentration was negligible so almost all the NO_x was as NO.
385 Inlet air flow, fuel input and furnace pressure were monitored continuously and stayed reasonably
386 constant throughout the experiments. The variation in the CO_2 and O_2 concentrations was due to
387 periodic collapses within the bed, due to the movement of the grate steps which move the fuel along
388 the grate, combined with the effect of fuel shrinkage during burnout. As these collapses occur, they
389 expose additional unburnt fuel surface area within the bed to the combustion air and increase CO_2
390 production rate, as these particles burn out the CO_2 starts to drop. There is a minimum O_2
391 concentration under which the CO formation increases significantly and consistently for this boiler.
392 The boiler was operated close to the O_2 limit to maximise CO_2 concentration in the flue gas.
393 Particulate concentrations were measured both downstream of the ESP and upstream of the
394 absorber while CO concentration was measured at the absorber inlet. Generally, higher the CO,
395 higher the soot. However, the correlation between CO and dust concentrations weren't part of the
396 scope of this study so no effort was made to establish a correlation.
397 Figure 6 plots CO_2 concentration in the absorber inlet and outlet flue gases for a typical operational
398 day. As can be observed from the figure that outlet CO_2 followed the same trend as the inlet and any
399 variation in the inlet CO_2 concentration was quickly realised in the outlet gas. The reason for this
400 could be the short residence time in the RPB absorber. In the conventional absorber the impact of
401 inlet CO_2 variation is dampened to some extent due to higher residence times. Moreover, this could
402 be less of a problem at commercial scale plants as, from a legislation point of view, it is the average
403 capture efficiency which is more important rather than instant values. Nevertheless, the flue gas
404 composition variation makes it hard to adjust the capture plant to a specific capture efficiency.
405 Figure 5: Gas composition at the absorber inlet
406 Figure 6: CO_2 concentration at the inlet and outlet of absorber

4.2.2 Solvent degradation (35wt% MEA)

One of the main challenges with the absorption-based CO_2 capture process is solvent degradation and corrosion. Corrosion rate can be influenced by process conditions, plant material, plant section, solvent concentration, CO_2 concentration, dissolved oxygen [21] as well as impurities in the flue gas being treated. Loss of MEA due to degradation could be very high, 2.4 kg of MEA per ton of CO_2 captured [22] or even up to 3.6 kg of MEA per ton of CO_2 captured [23] depending upon the operational conditions and flue gas characteristics. Oxidative degradation mostly happens in the absorber sump [24] is responsible for around 95% degradation of MEA [25] and is accelerated by the presence of metal ions [26-28].

Biomass contains volatile metals which can be transported to the solvent system via small particulates and can contribute to solvent degradation. Therefore, particulates concentrations were measured at the boiler exit and absorber inlet. Particulates samples were collected, and post analysed for metallic content. Furthermore, solvent samples were also collected frequently and were analysed for build-up of some common metals and anions.

Rate of ammonia emissions in the absorber exit gas can be directly related to the rate of solvent degradation. In the following sections, ammonia emissions, particulates measurements and metallic content, accumulation of metals in the solvent and their potential impact on the solvent degradation are discussed.

4.2.2.1 Ammonia emissions

Ammonia is a degradation product of MEA. A clear correlation between ammonia emissions and metal concentration has been observed during pilot scale test campaigns [25,29]. Therefore, emissions of ammonia are monitored and are considered to be a way of monitoring rate of degradation in CO_2 capture plants. Higher the emissions of ammonia, higher the rate of degradation. The rate of degradation is influenced by many factors, one of them is oxygen content of the flue gas to be thought of responsible for oxidative degradation. The rate of degradation is enhanced by the

presence of certain impurities in the flue gas as well as metals from the construction material. These are further discussed in the following sections.

Figure 7 plots oxygen concentration in the absorber inlet flue gas and ammonia emissions at the outlet of absorber. It can be observed that the oxygen content in the gas has a direct impact on the ammonia emissions and both follow the same trend. Most of the data is very consistent indicating increase in oxygen content of the flue gas results in increased ammonia emissions. However, it is worth noting that ammonia emissions were always below 25 ppm.

The reason for increase in ammonia emissions from 6ppm to 12ppm is not known. It is understood that oxidative solvent degradation is caused by the presence of oxygen but is accelerated by other factors such as operational conditions, presence of dissolved metals etc. Therefore, it cannot be concluded that all the ammonia is emitted due to the effect of oxygen alone due to the involvement of other factors.

The relatively low ammonia emissions indicate slow rate of degradation. Losses of MEA due to degradation during the test campaign are estimated to be 1.1 kg/t CO_2, considerably lower than 2.4 kg/tCO_2 measured by [22] during CO_2 capture from coal flue gas. This might be due to short duration of the tests (116 hrs) and the solvent was not significantly degraded over the test period. Moreover, the tests were started with fresh MEA (35%) solvent and the solvent inventory was maintained by the plant control system by transferring water from water wash for compensating water losses.

Figure 7: Impact of flue gas oxygen content on ammonia emissions

4.2.2.2 Particulate measurements:

Particulates can carry volatile metals which can have detrimental impact on the solvent. The level of particulates in the flue gas depends upon many factors such as boiler technology, gas treatment system as well as length of flue gas path between the source and capture plant.

The data measured with the Dekati ELPI®+ particulate analyser is presented in Figure 8 for number, size and mass distribution as a function of particle aerodynamic diameter. Due to small number of particulates at the absorber inlet, it took around ~4 hrs to collect reasonable amount of sample for

458 analyses. The data presented for metallic concentrations of the particulate samples can be considered
459 as averaged over the sample collection period as whole of the collected sample was digested and
460 analysed.
461 As can be noted that the plot only shows up to PM1 particles as in the case of particle measurements
462 at the absorber inlet, plate no 10 (>PM1) did not record any particles due to an error in the analyser.
463 It can be observed from the Figure that some of the bigger particles observed at the boiler exit did
464 not reach the absorber inlet and likely attached to the pipe walls due to several factors including
465 impact to walls wetted by condensation in the pipework. Average mass of particulates at the boiler
466 exit was 21.6 mg/m^3 while at the absorber inlet it was 1.5 mg/m^3, indicating that ~93% of
467 particulates mass was lost in the pipework. Particle number distribution shows that a large number
468 of very small particles was present at the inlet to the absorber. This is likely due to the formation and
469 growth of volatile particulate matter and aerosols formation as the exhaust cools down in the
470 pipeline resulting in condensation. However, it should be noted that the measurements at the boiler
471 exit, and absorber inlet were performed on different days, so the above explanations are not
472 conclusive, however the boiler operational conditions on both days were the same so particulates
473 characteristics should not be significantly different. Nevertheless, the data highlights that significant
474 number of particulates can enter the solvent system via the flue gas and can have impact on the
475 solvent.
476 Figure 8: Particulates size and number distribution at grate boiler exit and absorber inlet
477 Average particulates mass concentration of 22 mg/m^3 at the boiler exit (after ESP) during the tests
478 was considerably lower than the limits 50 mg/m^3 imposed by the MCPD [30]. However, the particle
479 mass concentration dropped to 1.5 mg/m^3 at the inlet to the absorber. Particles in the form of soot
480 can result in increased MEA emissions due to possibility of formation of aerosols. Khakharia et al.
481 2013 [31] did aerosol formation experiments using aerosol generator capable of producing
482 controlled amounts of soot and dosing sulphuric acid aerosol to a mobile CO_2 capture mini-plant.
483 They observed that soot particles having a number concentration in the order of 10^4/cm^3 and

484 $10^6/cm^3$ resulted in MEA emissions in the order of 35 and 70 ppmv, respectively. During this study
485 average particulates mass and number concentrations were 1.5 mg/m^3 and $1.07x10^6/cm^3$,
486 respectively which resulted in average MEA emissions of ~80 ppmv, which is not far from that
487 measured by Khakharia et al. [31]. The maximum flue gas temperature (35 ^oC) measured near the
488 flue gas sampling location was also close to that measured by Khakharia et al., 34 ^oC [31]. Although
489 the average particle number during this study was similar to that measured by Khakharia et al. [31],
490 smaller particles in the range of 0.012 µm were considerably higher in the order of $2.5x10^6/cm^3$.
491 Therefore, MEA emissions are expected to be much higher than those measured by Khakharia et al.
492 [31]. However, the absorber exit gas sampling point in this study was ~6m away from the absorber so
493 it is possible that MEA vapours may have been condensed in the unlagged pipework and separated
494 from the flue gas in the u-bend before the sampling point.
495 Twence waste to energy plant measured relatively higher MEA emissions of 150-400 mg/Nm^3 with
496 slightly higher particulates concentration at the absorber inlet, in the range of $3.4x10^7$ $/cm^3$- $1.2x10^8$
497 $/cm^3$ [32]. The data highlights that higher particulates concentration at the absorber inlet can
498 potentially result in increased MEA emissions. A Brownian Demister Unit (BDU) installed at the
499 absorber inlet was affective in removing up to 99% of the particulates entering the absorber and
500 emissions of MEA were dropped to below 15 mg/Nm^3 reference limit [32].
501 The intensified CO_2 mass transfer into the solvent can result in elevated temperatures in the RPB due
502 to exothermic reaction and thus higher absorber exit gas temperatures. This can result in higher carry
503 over of solvent potentially needing better wash columns designs to cool the gas and efficiently remove
504 carried over solvent. During this study, however, due to the absorber gas sampling point considerably
505 away from the absorber, the impact on the carry over solvent was not considerable and most of the
506 liquid condensed in the pipe work. The existing water wash was able to remove most of the carried
507 over solvent.

4.2.2.3 Particulates sample analyses

It can be observed from Table 1 that Calcium, Potassium, Sodium, Aluminium, Magnesium, Phosphorus and Iron were present in significant amounts in the biomass. The metals can enter the capture plant solvent as sub-micron particles. It is not fully understood how the presence of different metals impacts the solvent degradation behaviour. However, it is observed that presence of Iron which is also present in Stainless Steel can cause significant solvent degradation. Therefore, particulate samples and MEA solvent samples were collected and analysed to investigate the impact of the metals on the solvent.

Particulate samples were collected at the boiler exit and absorber inlet, and are analysed at the laboratories at Leeds University by ICP-MS. The results are presented in Table 3. The table shows the amount of various metals in mg/kg of sample collected at different ELPI analyser plates, characterised by plate Di (µm). Some of the plates (Di = 0.022 µm and below; Di = 2 µm and above) did not collect enough sample so were not analysed. Also, during the sampling at absorber inlet, particulate analyser plate no. 10 (Di = 1.238 µm) had some technical issues and did not log any particles.

The data indicates that significant amounts of K, Zn, Na, Si, Fe, Mn were present in the particulate samples. Moreover, the amount of metals in particulates collected on different plates (Di) vary. Generally, highest amount is present in the middle plates. Some of the metals (Hg, P, S, Zr and Pd) were below the detection limit of the analyser. Also, Ti and V were mostly below the detection limits. Although Ca was in the highest concentration in the biomass sample analysis, it was not the highest in the particulate samples. On the other hand, K was present in the highest amounts followed by Zn, Na and Fe. The reason for relatively lower concentration of Ca in the particulates samples could be that CaO reacts with HCl to form $CaCl_2$ at the flue gas conditions by the following reaction [33].

$$CaO\ (s) + HCl\ (g) \rightarrow CaCl_2\ (s) + H_2O\ (g)$$

$CaCl_2$ is hygroscopic in nature and as flue gases contain significant amounts of moisture, $CaCl_2$ can form hydrates which at low temperatures can completely dissolve and form an aqueous solution by a

534 phenomenon called deliquiescence [34] well known in the deposits induced corrosion in the boiler
535 industry. This phenomenon may have resulted in some of the Ca to be dissolved and settled in
536 different sections of the boiler and the pipework. This hypothesis is also supported by negligible HCl
537 presence in the flue gas at the inlet to the absorber.

538 Table 3: ICP-MS results of particulate samples (mg/kg)

Boiler exit								
Plate no.	3	4	5	6	7	8	9	10
Di (µm)	0.0316	0.0577	0.103	0.18	0.296	0.47	0.757	1.265
K (39)	360939	355561	180591	44130.1	19400	6467.9	4327.5	999.7
Na (23)	12898.1	16891.5	14599.3	5242	1233.9	358.3	220.3	63.6
Zn (66)	27211.2	25520.8	20181.8	8301.8	1632.1	455.7	294.5	96
Fe (56)	15597.8	4641.8	1090.9	160.7	187.9	81.3	91.7	73
Li (7)	<LOD	82.7	65.9	23.4	6	1.8	1.2	0.4
B (11)	268.2	196.8	23.3	4.7	2.1	3.5	3.9	2.4
Mg (24)	<LOD	1222.2	153.4	54.8	22.5	31.3	68.6	108
Al (27)	<LOD	2223.6	145.8	41	<LOD	<LOD	<LOD	<LOD
Si (28)	181638	56248.3	4898.7	849.3	819.3	758.2	915.2	541.1
P (31)	<LOD	<LOD	1637	336.4	<LOD	<LOD	<LOD	<LOD
Ca (43)	<LOD	12075.9	567.6	140.4	204.3	264.1	350	622.3
Ti (48)	<LOD	<LOD	<LOD	39	<LOD	<LOD	<LOD	2.7
V (51)	<LOD	<LOD	1.2	<LOD	0.2	<LOD	<LOD	<LOD
Cr (52)	2761.2	755.3	261.6	46	45.4	15.4	12.6	10.6
Mn (55)	1563.2	1128.4	898.5	305.6	73.5	27.7	34.3	33.2
Co (59)	13.2	3.4	2	0.4	0.5	0.1	0.1	0.1
Ni (60)	1541.8	191.3	70	169.9	16	4.7	5.6	3.6
As (75)	<LOD	<LOD	31.3	13.8	2	<LOD	<LOD	<LOD

Sr (88)	<LOD	47.2	13.1	4.3	1.3	1	2.4	3.5
Cd (111)	165.5	145.5	104.1	39.1	9	2.9	1.9	0.6
Sn (118)	<LOD	31.2	27.7	9.2	2.6	0.5	0.4	0.3
Absorber inlet								
Plate no.	3	4	5	6	7	8	9	10[$]
Plate Di (μm)	0.02	0.032	0.057	0.111	0.213	0.419	0.734	1.238
K (39)	649084	784153	276575	91869.2	34867	15793	4967.6	-
Na (23)	29952.4	42059.6	14609.6	4775.2	1737.6	762.1	282.3	-
Zn (66)	50174.1	68869.7	25776.8	7879.6	2911.8	1178.4	403.4	-
Fe (56)	5186.6	3141.9	1659.1	251.6	966.3	68.2	1333	-
Li (7)	214.2	290.3	104.6	33.3	13.1	5.5	1.8	-
B (11)	<LOD[*]	<LOD	30.2	20.4	<LOD	2.6	3.6	-
Mg (24)	<LOD	552.6	278.1	74.6	32.5	18.9	37.8	-
Al (27)	1652.2	<LOD	499.2	<LOD	41	<LOD	98.3	-
Si (28)	31359.8	9849.3	5358.1	1515.1	300.7	854.8	540	-
P (31)	<LOD	<LOD	<LOD	<LOD	<LOD	<LOD	<LOD	-
Ca (43)	<LOD	<LOD	3178.1	726.9	213.3	91.1	466.6	-
Ti (48)	<LOD	117.1	180.9	<LOD	15.2	3.2	34.3	-
V (51)	<LOD	<LOD	3.4	1.1	0.5	<LOD	<LOD	-
Cr (52)	1367.1	828.1	388.8	71.2	34.3	19.3	9	-
Mn (55)	2468.5	3260.4	1164.1	377.7	129.6	60.9	26.8	-
Co (59)	10.4	5.7	4.5	0.6	0.2	0.2	0.5	-
Ni (60)	333.6	154.1	51.3	42.2	<LOD	26	671.1	-
As (75)	184.3	215.5	57.3	16.5	5.6	3.2	<LOD	-
Sr (88)	43.5	57.1	23.2	6.8	2.4	1.4	2.2	-

Cd (111)	167.8	227.2	83.2	27.1	11.2	4.6	1.4	-
Sn (118)	88	192	46.1	13.3	5.3	2.4	0.9	-

539 *LOD - Level of Detection; $ - Plate no. 10 for boiler exit measurements developed a fault and did not record particles

540 Figure 9: K, Zn, Na and Fe in particulate samples at boiler exit and absorber inlet

541 Figure 10: Percentage loss of metals between boiler and absorber

542

543 Figure 9 plots the metals found in the highest quantities in the particulates i.e. K, Zn, Na, Ca, Mg and
544 Fe at the boiler exit and absorber inlet as a function of particle diameter. As can be observed from
545 the Figure that only PM1 particles are reported due to the reason that the analyser did not record
546 any particles bigger than PM1 (Plate no. 10) in the case of measurements at the absorber inlet. The
547 figure shows that the magnitude of K is around ten times higher than Zn, the next highest. The figure
548 highlights that most of the metals were present in the smaller particles. The figure also indicates
549 that a significant mass of the metals was lost between the boiler and the absorber. The mass of
550 metals lost between the boiler exit and absorber inlet varies ranging between 70 and 90% for most
551 of the metals, see Figure 10. The loss varies from 40% for Ni to 100% for P which was below the
552 detection limit at the absorber inlet.

553 #### 4.2.2.4 Solvent analysis

554 In order to investigate the impact of volatile metals present in biomass on the solvent degradation,
555 rich and lean solvent samples were collected at the end of each day and were analysed using ICP-OES
556 for a number of metals present in biomass and construction material (Stainless steel). The results
557 were similar for both of the samples so only lean samples analysis are presented here, Figure 11. It
558 can be observed from the Figure that there was a significant presence of Potassium, Calcium and
559 Sodium metals which are also present in significant amounts in biomass, see Table 1. Potassium was
560 found to be in the highest amount in the solvent samples, followed by Na, Ca and Fe. Zn was found
561 to be lower in the solvent samples while was relatively high in the particulate samples. ZnO is

562 insoluble in water and MEA while $ZnCl_2$ is soluble in both water and MEA. Therefore, it is possible
563 that most of the Zn in the particulates was present as ZnO and settled in the capture plant.
564 Potassium tends to increase over time although rate of increase slowed down towards the end,
565 however, Sodium and Calcium did not show much change over the test period. Potassium and
566 Sodium are normally present in fly ash as K_2O and Na_2O both of which can react with water to form
567 respective hydroxides. The hydroxide, KOH and NaOH, both are used for CO_2 capture. The reason for
568 continued increase in potassium but steady concentration of sodium over the test period needs
569 further investigation. Part of the reason could be that the total amount of potassium in the
570 particulates at the absorber inlet was ~20 times higher as compared to Sodium. Other metals such as
571 Fe, Mg etc. are also found in small amounts but were below 2 mg/kg at the end of the test campaign.
572 The presence and accumulation of some of these metals may accelerate or inhibit solvent
573 degradation [35-43] resulting in plant corrosion and thus increasing operational costs as well as
574 costly equipment replacement.
575
576 Table 4: Critical metals accumulation

		Cu	Cr	Ni	Fe	V
Absorber inlet	mg/kg of particulates (average of all the plates)	-	388.3	213.1	1800	1.66
	Cumulative (mg) over the test period (116 hrs)		10.13	5.56	46.98	0.04
Solvent	mg/kg of solvent (last sample at 116 hrs)	0.08	0.25	0.15	1.85	
	Cumulative (mg) in total solvent inventory (450 kg)	36	112.5	67.5	832.5	
%age from flue gas			9	8.2	5.6	-

577

578 Table 4 shows cumulative content of some of the critical metals at absorber inlet and in the solvent.
579 The data presented in table 4 indicates that even if all the metals in the flue gas entering the
580 absorber were to dissolve in the solvent the contribution from the flue gas is less than 10%. Schallert
581 et al. 2014 [40] reported that particulates undergo leaching with MEA solution to a small extent
582 indicating that the contribution of metallic content from the biomass flue gas into the solvent may
583 have been even less than those calculated in the table assuming that 100% of the metallic content in
584 the particulates entering the absorber is dissolved in the solvent. This highlights that majority of the
585 metals were from metal corrosion from the plant potentially caused by the presence of heat stable
586 salts [44] rather than from the biomass flue gases. The order of magnitude of the metals is also
587 similar to that in SS304, Fe>Cr>Ni.
588 Clery et al. [45] during lab tests highlighted that metals present in the biomass ashes were also
589 present in the solvent. However, the amounts of metals present in the solvent during the current
590 pilot scale demonstration were not in line with the quantities present in the biomass or particulates
591 sampled at the absorber inlet but, as mentioned earlier, mostly seem to be coming from the plant
592 corrosion.
593 Figure 11: ICP-OES analysis of MEA samples
594 The solvent samples were also analysed for build-up of anions, using Ion Chromatography, Figure 12,
595 for the presence and accumulation of these degradation products [46-50]. Formate, was observed to
596 be present in highest amounts (~70 ppm) followed by nitrate (~27 ppm), and nitrite (~22 ppm).
597 Oxalate was found to be very low (~2 ppm).
598 Comparing data from different pilot scale test campaigns Buvik et al. [46] found that acetate and
599 formate were dominant degradation products, but the order of magnitude was different based on
600 process conditions. The average concentration of formate, acetate and oxalate was found to be 2500,
601 800 and 500 mg/kg per 1000 hrs, respectively. However, most of these studies were on coal and
602 some on gas combustion but none was on biomass. Rieder et al. [51] observed that formate ions
603 were typically the most abundant HSS at pilot scale. Same observation was made by Buvik et al. [43]

and observed that formate, acetate and oxalate made almost half of the HSS content. The current data indicates that the ratio of acetate to formate was in the order of 4 comparable with that reported by [52] who measured 5 times acetate as compared to formate. However, [53] reported acetate to formate ratio of 1/5 at Technology Centre Mongstad test campaign.

Figure 12 highlights that during current study, formate and acetate concentrations dropped after 90 hrs of operation with acetate seeing a big drop. As the boiler conditions were the same and same biomass was used, the oxygen content or the biomass composition is not expected to change significantly. Therefore, it is likely that these species reacted with MEA and other degradation products to from organic HSS [47]. Concentrations of nitrate and nitrite seem to be steady and below 30 ppm until the end of the test campaign. It is possible that nitrite and nitrite were being produced and also consumed and converted to other species during the process. Formaldehyde can reduce nitrate to nitrite and ultimately to nitrogen gas in the presence of metal catalyst [54]. Reduction in nitrate concentration around 80 hrs may also be due to the same phenomenon.

Total accumulation of measured HSS during this study over the 116 hrs operational period was 163 ppm, at a rate of 1.4 ppm/h. Thompson et al. [55] observed HSS accumulation at a rate of 48 ppm/hr over 200 hrs in 30% MEA which is around 34 times higher than the current study. Threshold for HSS has been reported to be up to 0.5% of the weight of the solvent as benchmark to assess purification requirements of the solvent to remove HSS and other degradation products [56]. The threshold levels for oxalate and formate are 250 and 500 ppm, respectively [47]. These thresholds were never reached during the current tests, likely due to short duration but the concentrations of the HSS observed were not increasing at an alarming rate. However, there will be some point after which solvent will have to be purified using methods such as thermal reclaiming or by removing HSS and other degradation products by methods such as ion exchange membranes. These will increase operational costs and may results in solvent loss and further degradation during the process [55]. Therefore, a balance need to be established at which point and to what extent the solvent need to be cleaned or purified to optimise the process and minimise costs.

630 During the present study after 116 hrs of operation, total HSS accumulation of the measured species
631 was 0.005% considerably lower than those reported in literature. Thompson et al. [55] and Knudsen
632 et al. [57], observed 1% and 0.75%, respectively, HSS accumulation over 200 hrs of operation in 30%
633 MEA. Gao et al. [58], in pilot scale experiments reported HSS accumulation rate of 0.2% and 0.4%
634 after 100 and 200 hrs, respectively. Similarly, Wilson et al. [59] reported accumulation of HSS at a
635 rate of 0.4% at Sask power Boundary Dam plant. It has been recommended to use solvent
636 management techniques such as reclaiming if concentration of HSS exceeds 1.5wt% [60].
637 The relatively lower HSS accumulation during the current study could be due the presence of K, Ca
638 and Na metals in the biomass flue gas which accumulate in the solvent and can act as degradation
639 inhibitors for MEA [43]. This indicates that removal of metals from the flue gas has to be prioritised
640 carefully. Therefore, it is required to enhance the flue gas cleaning requirements to remove the
641 elements which are detrimental to the solvent before entering the solvent system. Once they are
642 part of the solvent system, the cleaning requirements are different. Solvent reclaiming options are
643 being investigated to keep the solvent relatively clean using different techniques such as thermal
644 reclaiming but these investigations are at early stages. Generally, plant operation should be
645 controlled to maintain suitable conditions to reduce solvent degradation.
646 The current study demonstrated BECCS experimentally in the real industrially relevant environment
647 using real biomass flue gases. However, the tests were of short duration (116 hrs), and therefore it is
648 not possible to investigate degradation trends thoroughly. However, the data acquired can provide
649 useful insight for further studies on the solvent degradation by biomass flue gases. Longer term tests
650 with real biomass flue gas and modelling of degradation chemistry are required to better understand
651 the impact of contaminants in biomass flue gases on the behaviour of solvent in the CO_2 capture
652 plants.
653 Figure 12: Anion concentrations in solvent samples

5 Conclusions:

Bioenergy with CCS can play a vital role in providing negative CO_2 emissions required to meet net zero targets by 2050. However, the impact of biomass flue gas on the solvent behaviour is far from understood. Longer term tests with real biomass flue gas are required to better understand the impact of biomass flue gas contaminants on the solvent behaviour. Based on the data presented here, following conclusions can be drawn.

Flue gas composition varied significantly requiring more time to achieve steady state on the capture plant. However, depending upon the design of the boiler combustion control system, this issue may be less pronounced at commercial scale and can be overcome by averaging the data over longer periods. Nevertheless, boiler control systems should be designed to provide flue gas composition as consistent as possible to precisely quantify the energy consumption for stripping CO_2 in the capture plant and to optimise the process.

Capture efficiency and reboiler duty varied as a function of L/G ratio and minimum reboiler duty was found at L/G = ~2 where capture efficiency was around 85%.

To achieve maximum benefit, rich loadings should be close to theoretical maximum value, 0.5 mol/mol for MEA. However, CO_2 loadings measurements have indicated that maximum rich loading under the operational conditions was ~0.4 mol/mol. Thus, the data highlights that the current RPB absorber design requires modification to achieve higher rich loadings. Moreover, the reason for lower rich loading in the RPB absorber appears to be short residence time, and it is anticipated that it may perform better with more reactive solvents than MEA.

Particulate measurements at the boiler exit and absorber inlet has shown that ~93% of the particulates by mass were lost in the pipework and did not reach the capture plant. Most of the lost particles were larger particles as can be expected. Further investigations are needed to understand this strong effect in this testing facility.

Significant amount of Potassium was observed in the particulate's samples collected at the absorber inlet and in the solvent samples. Similarly, Sodium was also present abundantly at both places, in

680 particulates and in solvent. However, Zn was relatively low in the solvent samples although was present
681 in significant amounts in particulate samples.
682 Formate, nitrate, nitrite and acetate were found in significant quantities in the solvent samples, while
683 oxalate concentration was very low (<2ppm). The data indicates that solvent degraded relatively
684 quickly at the start, within ~20 hrs, but was relatively stable after that over the test period. As the tests
685 were of only 116 hrs duration, it is possible that degradation could have been increased if the tests
686 were to continue.
687 It is not possible to quantify the impact of volatile metals on the solvent degradation due to the
688 involvement of several factors, but it is understood that presence of some metals in the solvent
689 catalyse the degradation process while some metals act as degradation inhibitors. Therefore, solvent
690 management techniques should be designed to reduce solvent losses due to overcleaning and to
691 control the process in such a way that only species are removed which are detrimental to the process.
692 This may require multiple technologies in series.
693 The test campaign was relatively short due to budget limitations. Therefore, it is anticipated that the
694 accumulation of flue gas contaminants and degradation products has not reached saturation and
695 interaction of degradation products/dissolved metals with the solvent was limited [52]. However, the
696 data presented here can serve as a starting point for further investigation in this field. Longer term test
697 campaigns with more rigorous analysis are required to better understand the interactions between
698 different species in the solvent system and threshold concentration of the species for triggering
699 accelerated degradation.

700 6 Acknowledgement

701 The authors want to acknowledge the financial support provided by Industrial Decarbonisation
702 Research and Innovation Centre (IDRIC) to conduct this research work under Wave 2 projects call
703 (IDRIC project ID MIP6.6). Experimental facilities of the Energy Innovation Centre (EIC) at the University

of Sheffield, funded by European Regional Development Fund (ERDF) and Department for Energy Security and Net Zero (DESNZ) have been used for the experimental work.

7 References:

1. IEA, Going carbon negative: What are the technology options?, IEA, January 31, 2020. https://www.iea.org/commentaries/going-carbon-negative-what-are-the-technology-options [accessed 17/04/2025]
2. Drax, 2025, https://www.drax.com/about-us/our-sites-and-businesses/drax-power-station/, [accessed 25/02/2025]
3. Lu S, Fang M, Li Q, Chen H, Chen F, Sun W, et al., The experience in the research and design of a 2 million tons/year flue gas CO2 capture project for coal-fired power plants, International Journal of Greenhouse Gas Control, 2021, 110, 103423. https://doi.org/10.1016/j.ijggc.2021.103423
4. Ramshaw C and Mallinson RH, Mass transfer process. Patent No. 4,283,255. United States: United States Patent, Aug. 11, 1981.
5. Jassim MS, Rochelle G, Eimer D, Ramshaw C, Carbon dioxide absorption and desorption in aqueous monoethanolamine solutions in a rotating packed bed. Industrial Eng. Chem. Res. 2007, 46 (9), 2823–33. https://doi.org/10.1021/ie051104r
6. Lin C-C, Chen Y-S, Liu H-S, Prediction of liquid holdup in counter current-flow rotating packed bed. Chem Eng Res Des 2000; 78 (3), 397–03. https://doi.org/10.1205/026387600527293
7. Lin C-C, Liu W-T, Tan C-S, Removal of carbon dioxide by absorption in a rotating packed bed. Ind Eng Chem Res 2003; 42 (11), 2381–6. https://doi.org/10.1021/ie020669+
8. Cheng HH, Tan CS, Reduction of CO_2 concentration in a zinc/air battery by absorption in a rotating packed bed. J Power Sour 2006; 162:1431–6. https://doi.org/10.1016/j.jpowsour.2006.07.046

9. Pan S-Y, Chiang P-C, Chen Y-H, Tan -CS, Chang E-E, Ex situ CO_2 capture by carbonation of steelmaking slag coupled with metalworking wastewater in a rotating packed bed. Environ Sci Technol 2013, 47, 3308–15. https://doi.org/10.1021/es304975y
10. Nascimento JVS, Ravagnani TMK, Pereira JAFR, Experimental study of a rotating packed bed distillation column. Braz J Chem Eng. 2009, (26) 219–26. https://doi.org/10.1590/S0104-66322009000100021
11. Chamchan N, Jia-Yu C, Hsiao-Ching H, Jia-Lin K, Hill WDS, Shi-Shang J, et al., Comparison of rotating packed bed and packed bed absorber in pilot plant and model simulation for CO_2 capture, Journal of the Taiwan Institute of Chemical Engineers 2017,73, 20–26. https://doi.org/10.1016/j.jtice.2016.08.046
12. Wu T-W, Hung Y-T, Chen M-T, Tan C-S, CO_2 capture from natural gas power plants by aqueous PZ/DETA in rotating packed bed, Separation and Purification Technology 2017, (186), 309–17. https://doi.org/10.1016/j.seppur.2017.05.040
13. Sheng M, Xie C, Zeng X, Sun B, Zhang L, Chu G, et al., Intensification of CO_2 capture using aqueous diethylenetriamine (DETA) solution from simulated flue gas in a rotating packed bed, Fuel 2018 (234), 1518–27. https://doi.org/10.1016/j.fuel.2018.07.136
14. Akram M, Gheit A, Milkowski K, Gale W, Pourkashanian M, Comparison of conventional and process intensified next generation RPB absorbers for decarbonisation of the steel industry, Fuel 2025, 388, 134484, https://doi.org/10.1016/j.fuel.2025.134484.
15. Zhao F, Cui C, Dong S, Xu X, Liu H, An overview on the corrosion mechanisms and inhibition techniques for amine-based post combustion carbon capture process. Sep. Purif. Technol. 2023, (304), 122091. https://doi.org/10.1016/j.seppur.2022.122091
16. Kittel J, Gonzalez S, Corrosion in CO_2 post-combustion capture with alkanolamines–a review. Oil Gas Sci. Technol. 2014, 69 (5), 915–29. https://doi.org/10.2516/ogst/2013161

17. François MHJ-J, Grimstvedt A, and Knuutila HK, Iron Solubility Measurements in Aqueous MEA for CO_2 Capture, *Ind. Eng. Chem. Res.* 2025, 64, 2318−28, https://doi.org/10.1021/acs.iecr.4c03980
18. Norizam NNAN, Szuhnszki J, Ahmed I, Yang X, Ingham D, Milkowski K, et al., Impact of the blending of kaolin on particulate matter (PM) emissions in a biomass field-scale 250 kW grate boiler, Fuel 2024, (374) 132454. https://doi.org/10.1016/j.fuel.2024.132454
19. Michailos S, Gibbins J, A Modelling Study of Post-Combustion Capture Plant Process Conditions to Facilitate 95–99% CO_2 Capture Levels from Gas Turbine Flue Gases. Frontiers in Energy Research 2022;10. https://doi.org/10.3389/fenrg.2022.866838
20. Wells J, Heely A, Akram M, Hughes KJ, Ingham DB, Pourkashanian M, Simulation and modelling study of a chemical absorption plant to evaluate capture effectiveness when treating high CO_2 content iron and steel industry emissions, Fuel, Volume 380, 15 January 2025, 133189.
21. Chandan P, Richburg L, Bhatnagar S, Remias JE, Liu K, Impact of fly ash on monoethanolamine degradation during CO_2 capture. International Journal of Greenhouse Gas Control 2014, 25, 102–108. https://doi.org/10.1016/j.ijggc.2014.03.015
22. Knudsen JN, Jensen JN, Vilhelmsen, P-J, and Biede O, Experience with CO_2 Capture from Coal Flue Gas in Pilot-scale: Testing of Different Amine Solvents, Energy Procedia 2009, 1(1), 783–90. https://doi.org/10.1016/j.egypro.2009.01.104
23. Rieder A, CO_2-Abscheidung aus Kraftwerksrauchgasen mit wässriger MEA-Lösung - Waschmitteldegradation und Aufbereitungsverfahren, PhD thesis, University Stuttgart, Germany, 2016.
24. Goff GS, Rochelle GT, Monoethanolamine Degradation: O_2 Mass Transfer Effects under CO_2 Capture Conditions. Ind. Eng. Chem. Res. 2004, 43, 6400–8. https://doi.org/10.1021/ie0400245

25. Dhingra S, Khakharia P, Rieder A, Cousins A, Reynolds A, Knudsen J, et al. Understanding and Modelling the Effect of Dissolved Metals on Solvent Degradation in Post Combustion CO_2 Capture Based on Pilot Plant Experience. *Energies*. 2017; 10(5):629. https://doi.org/10.3390/en10050629
26. Goff GS, Oxidative Degradation of Aqueous Monoethanolamine in CO_2 Capture Processes: Iron and Copper Catalysis, Inhibition, and O_2 Mass Transfer. PhD theses, The University of Texas at Austin, May, 2005. https://sites.utexas.edu/rochelle/files/2015/02/Dissertation-PrintCopy-final-2sided.pdf
27. Bedell SA, Oxidative degradation mechanisms for amines in flue gas capture. Energy Procedia 2009, 1, 771–778. https://doi.org/10.1016/j.egypro.2009.01.102
28. Voice AK, Rochelle GT, Inhibitors of monoethanolamine oxidation in CO_2 capture processes. Ind. Eng. Chem. Res. 2014, 53 (42), 16222−28. https://doi.org/10.1021/ie500996z
29. Mertens J, Lepaumier H, Desagher D, Thielens ML, Understanding ethanolamine (MEA) and ammonia emissions from amine based post combustion carbon capture: Lessons learned from field tests. Int. J. Greenh. Gas Control 2013, 13, 72−77. https://doi.org/10.1016/j.ijggc.2012.12.013
30. EU Directive (2015), DIRECTIVE (EU) 2015/2193 OF THE EUROPEAN PARLIAMENT AND OF THE COUNCIL of 25 November 2015 on the limitation of emissions of certain pollutants into the air from medium combustion plants. ELI: http://data.europa.eu/eli/dir/2015/2193/oj
31. Khakharia P, Brachert L, Mertens J, Huizinga A, Schallert B, Schaber K, et al., Investigation of aerosol-based emission of MEA due to sulphuric acid aerosol and soot in a Post Combustion CO_2 Capture process, International Journal of Greenhouse Gas Control 2013, 19, 138–144. https://doi.org/10.1016/j.ijggc.2013.08.014
32. Monteiro J, Srivastava T, Ros J, Huizinga A, Gravesteijn P, Van Os P, Aerosol Emissions at a post combustion CO_2 capture plant at Twence (WtE facility), TCCS-11 - Trondheim Conference on CO_2 Capture, Transport and Storage, Trondheim, Norway - June 21-23, 2021.

803 33. Vainio E, DeMartini N, Hupa L, Åmand L-E, Richards T, Hupa M, Hygroscopic Properties of
804 Calcium Chloride and its Role on Cold-End Corrosion in Biomass Combustion. Energy Fuels
805 2019, 33(11), 11913–22. https://doi.org/10.1021/acs.energyfuels.9b02731
806 34. Ruozzi, A, Vainio E, Kinnunen H, Hupa L, Cold-end corrosion in biomass combustion – Role of
807 calcium chloride in the deposit, Fuel, 2023, (349) 128344.
808 https://doi.org/10.1016/j.fuel.2023.128344
809 35. Voice AK, Rochelle GT, Products and process variables in oxidation of monoethanolamine for
810 CO_2 capture . Int J Greenhouse Gas Control 2013, 12 : 472 –77.
811 https://doi.org/10.1016/j.ijggc.2012.11.017
812 36. da Silva EF, Lepaumier H, Grimstvedt A, Vevelstad SJ, Einbu A, Vernstad K, et al.,
813 Understanding 2-ethanolamine degradation in post-combustion CO_2 capture. Ind. Eng. Chem.
814 Res. 2012, 51, 13329–38. https://doi.org/10.1021/ie300718a
815 37. Voice AK, Amine Oxidation in Carbon Dioxide Capture by Aqueous Scrubbing , thesis.
816 University of Texas, Austin, TX, USA (2013).
817 38. Sexton AJ, Rochelle GT, Catalysts and inhibitors for oxidative degradation of
818 monoethanolamine. Int. J. Greenh. Gas Control 2009, 3(6), 704–11.
819 https://doi.org/10.1016/j.ijggc.2009.08.007
820 39. Reynolds AJ, Verheyen TV, Adeloju SB, Chaffee AL, Meuleman E, Primary sources and
821 accumulation rates of inorganic anions and dissolved metals in a MEA absorbent during PCC
822 at a brown coal-fired power station. Int. J. Greenh. Gas Control 2015, 41, 239–248.
823 https://doi.org/10.1016/j.ijggc.2015.07.004
824 40. Schallert B, Neuhaus S, Satterley CJ, Is Fly Ash boosting amine losses in carbon capture from
825 coal? Energy Procedia 2014, 63, 1944–56. https://doi.org/10.1016/j.egypro.2014.11.206
826 41. Skylogianni E, Figueiredo RV, van Os P, Frost J, Hall J, Yelland TS, et al., Demonstration of
827 solvent performance at an industrial WtE facility, 16th International Conference on

828 Greenhouse Gas Control Technologies, GHGT-16-23rd -27th October 2022, Lyon, France.
829 http://dx.doi.org/10.2139/ssrn.4286070
830 42. Vega F, Sanna A, Navarrete B, Maroto-Valer MM, Cortés VJ, Degradation of amine-based
831 solvents in CO_2 capture process by chemical absorption, Greenhouse Gases: Science and
832 Technology, vol. 4, no. 6. 2014. https://doi.org/10.1002/ghg.1446
833 43. Buvik V, Vevelstad SJ, Moser P, Wiechers G, Wanderley RR, Monteiro JGM, et al., Degradation
834 behaviour of fresh and pre-used ethanolamine, Carbon Capture Science & Technology 2023,
835 7, 100110. https://doi.org/10.1016/j.ccst.2023.100110
836 44. Tanthapanichakoon W, Veawab A, McGarvey B, Electrochemical Investigation on the Effect of
837 Heat stable Salts on Corrosion in CO_2 Capture Plants Using Aqueous Solution of MEA. Ind.
838 Eng. Chem. Res. 2005, 8, 2586–93. https://doi.org/10.1021/ie050575a
839 45. Clery DS, Mason PE, Barnes DG, Szuhanszki J, Akram M, Jones J, et al., The effect of biomass
840 ashes and potassium salts on MEA degradation for BECCS, International Journal of Greenhouse
841 Gas Control, 2021 (108), 103305. https://doi.org/10.1016/j.ijggc.2021.103305
842 46. Buvik V, Høisæter KK, Vevelstad SJ, Knuutila HK, A review of degradation and emissions in
843 post-combustion CO_2 capture pilot plants, International Journal of Greenhouse Gas Control
844 2021, 106, 103246. https://doi.org/10.1016/j.ijggc.2020.103246
845 47. Verma N, and Verma A, Amine System Problems Arising from Heat Stable Salts and Solutions
846 to Improve System Performance. Fuel Process. Technol. 2009, 90: 483– 489.
847 https://doi.org/10.1016/j.fuproc.2009.02.002
848 48. Nainar M, and Veawab A, Corrosion in CO_2 Capture Process using Blended
849 Monoethanolamine and Piperazine. Ind. Eng. Chem. Res. 2009, (48), 9299–06.
850 https://doi.org/10.1021/ie801802a
851 49. Sexton AJ, Rochelle GT, Reaction Products from the Oxidative Degradation of
852 Monoethanolamine. Ind. Eng. Chem. Res. 2011, 50, 667–673.
853 https://doi.org/10.1021/ie901053s

50. Moser P, Wiechers G, Schmidt S, Figuiredo RV, Skylogianni E, Monteiro JGM-S, Conclusions from 3 years of continuous capture plant operation without exchange of the AMP/PZ-based solvent at Niederaussem-Insights into solvent degradation management, International Journal of Greenhouse Gas Control, 2023, (126), 103894. https://doi.org/10.1016/j.ijggc.2023.103894
51. Rieder A, Dhingra S, Khakharia P, Zangrilli L, Schallert B, Irons R, et al., Understanding Solvent Degradation A Study from Three Different Pilot Plants within the OCTAVIUS Project, Energy Procedia Volume 114, July 2017, Pages 1195-1209. https://doi.org/10.1016/j.egypro.2017.03.1376
52. Moser P, Wiechers G, Schmidt S, Monteiro JGM, Charalambous C, Garcia S, Results of the 18-month test with MEA at the post-combustion capture pilot plant at Niederaussem – new impetus to solvent management, emissions and dynamic behaviour, International Journal of Greenhouse Gas Control 95 (2020) 102945.
53. Morken AK, Pedersen S, Kleppe ER, Wisthaler A, Vernstad K, Ullestad O, et al., Degradation and emission results of amine plant operations from MEA testing at the CO_2 Technology Centre Mongstad. Energy Procedia 114, 2017, 1245–1262.
54. Numata M, Mihara S, Kojima S, Ito H, Reduction of Sodium Nitrate Liquid Waste in Nuclear Reprocessing Plants, Waste Management Symposia, February 26-March 2 2006, Tuscon, AZ.
55. Thompson JG, Frimpong R, Remias JE, Neathery JK, Liu K, Heat Stable Salt Accumulation and Solvent Degradation in a Pilot-Scale CO_2 Capture Process Using Coal Combustion Flue Gas, Aerosol and Air Quality Research, 14: 550–558, 2014, https://doi.org/10.4209/aaqr.2013.05.0150
56. Rooney PC, Dupart MS, Bacon TR, Effect of heat stable salts on MDEA solution corrosivity: part 2, Hydrocarbon Processing 1997, 76 (4), 65-71.
57. Knudsen JN, Jensen, JN, Vilhelmsen P-J, Biede O, First year operation experience with a 1 t/h CO_2 absorption pilot plant at Esbjerg coal-fired power plant. In Proceedings of the European Congress of Chemical Engineering (ECCE-6), Copenhagen, Denmark, 16–20 September 2007.

58. Gao J, Wang S, Zhao B, Qi G, and Chen C, Pilot-scale Experimental Study on the CO_2 Capture Process with Existing of SO_2: Degradation, Reaction Rate, and Mass Transfer. Energy Fuels 2011, 25: 5802–9. https://doi.org/10.1021/ef2010496

59. Wilson M, Tontiwachwuthikul P, Chakma A, Idem R, Veawab A, Aroonwilas A, et al., Test Results from a CO_2 Extraction Pilot Plant at Boundary Dam Coal-fired Power Plant. Energy 2004, (29), 1259–67. https://doi.org/10.1016/j.energy.2004.03.085

60. Morken AK, Pedersen S, Nesse SO, Flø NE, Johnsen K, Feste JK, et al. CO_2 capture with monoethanolamine: Solvent management and environmental impacts during long term operation at the Technology Centre Mongstad (TCM), International Journal of Greenhouse Gas Control 82 (2019) 175–183.

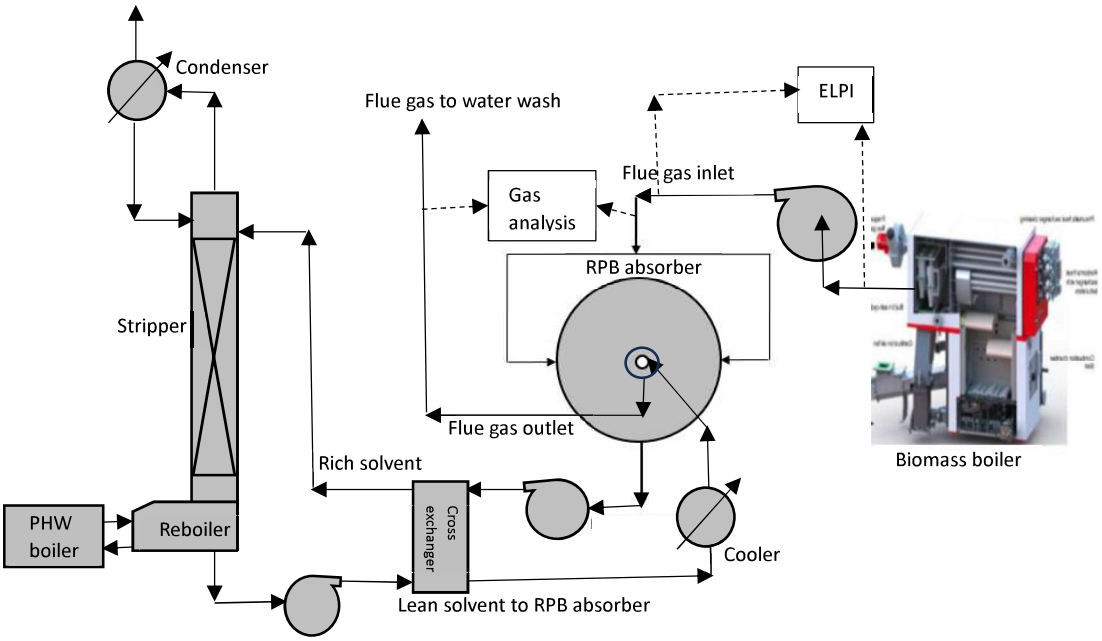

Figure 1a: Simplified experimental setup

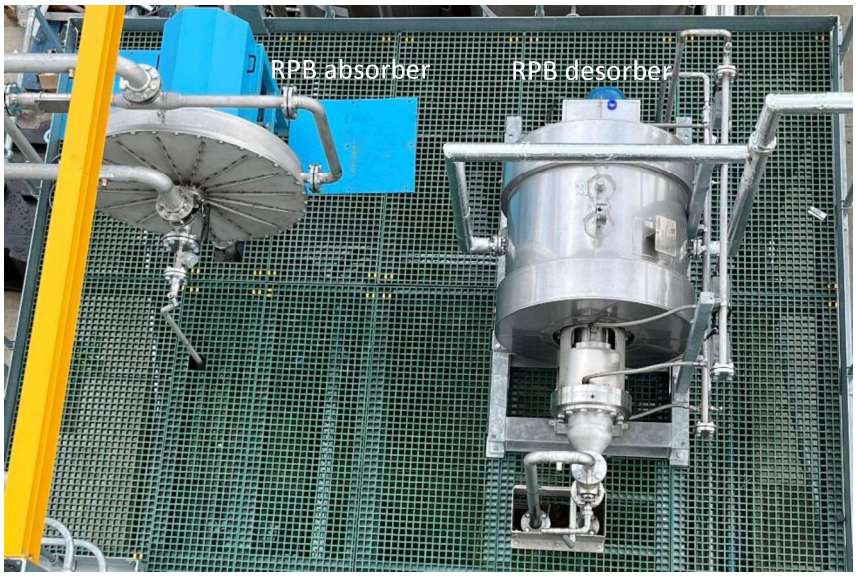

Figure 1b: RPB absorber and desorber

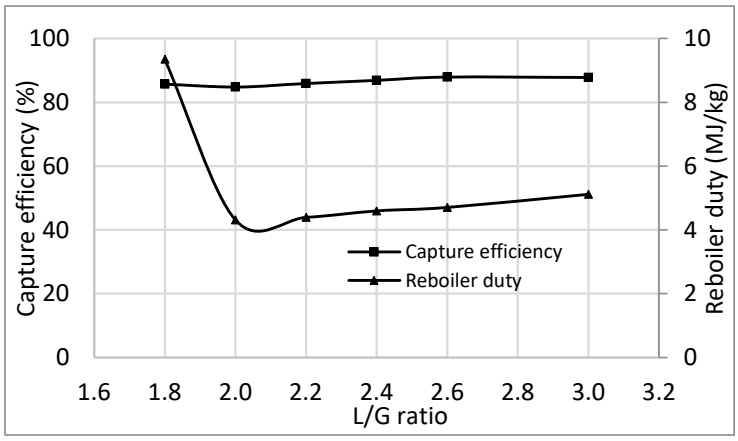

Figure 2: Capture efficiency and reboiler duty as a function of L/G ratio

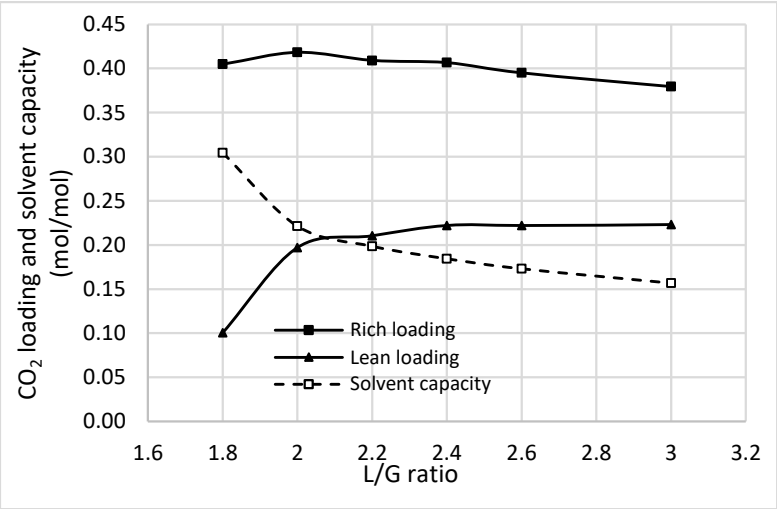

Figure 3: CO_2 loadings as a function of L/G ratio

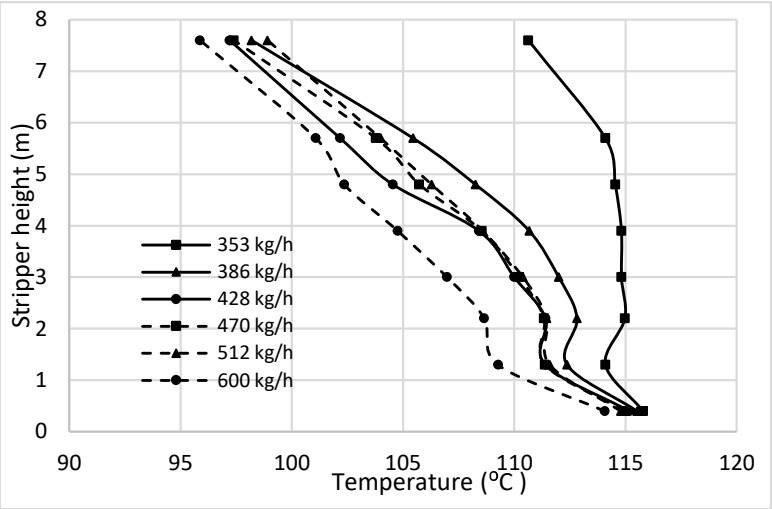

Figure 4: Stripper temperature profile for L/G ratio variation tests with MEA

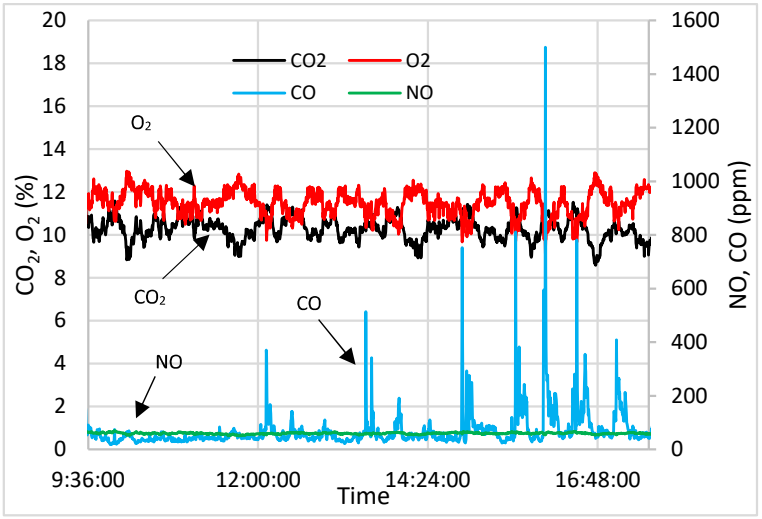

Figure 5: Gas composition at the absorber inlet

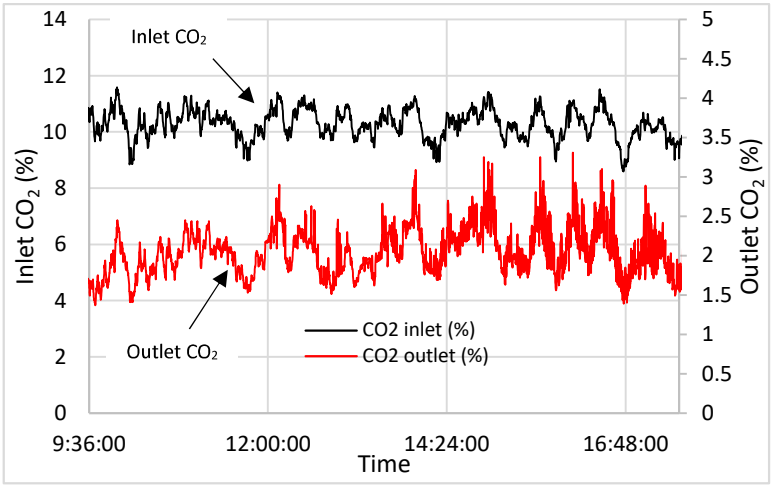

Figure 6: CO_2 concentration at the inlet and outlet of absorber

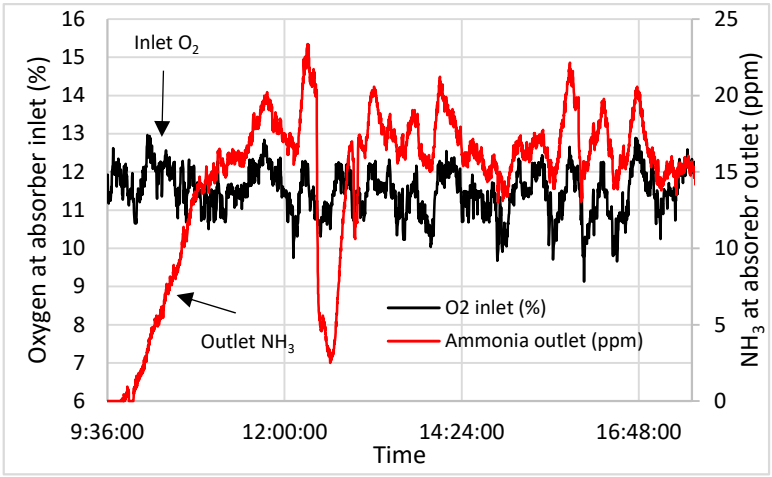

Figure 7: CO_2 concentration at the inlet and outlet of absorber

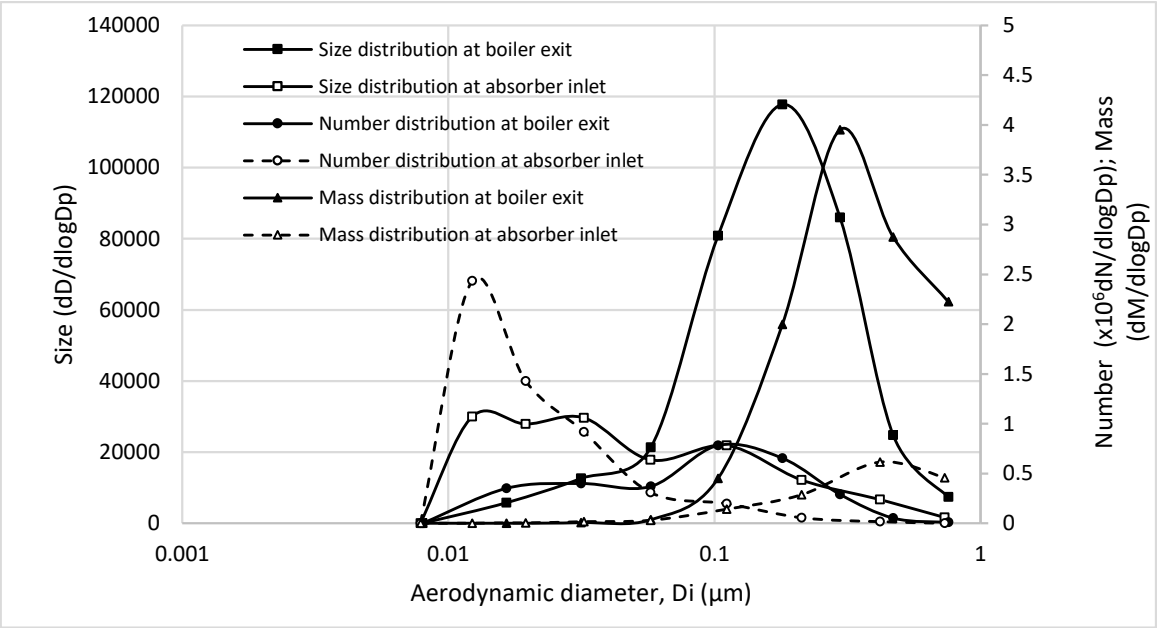

Figure 8: Particulates size and number distribution at grate boiler exit and absorber inlet

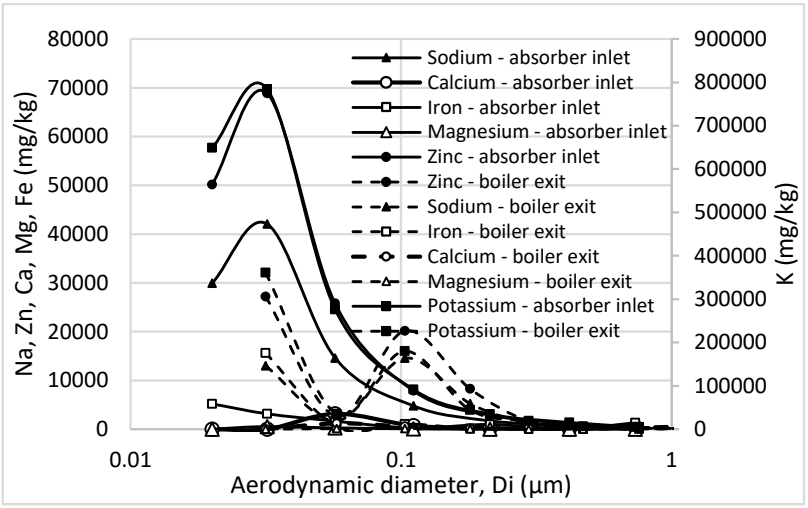

Figure 9: K, Zn, Na and Fe in particulate samples at boiler exit and absorber inlet

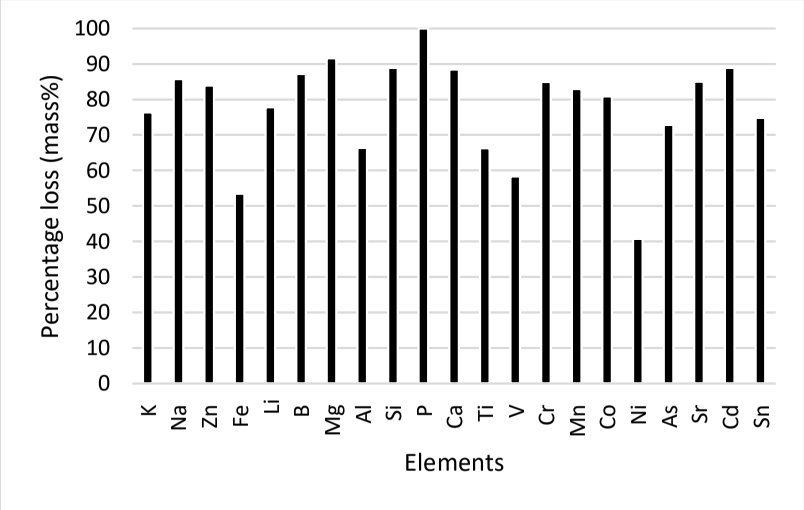

Figure 10: Percentage loss of metals between boiler and absorber

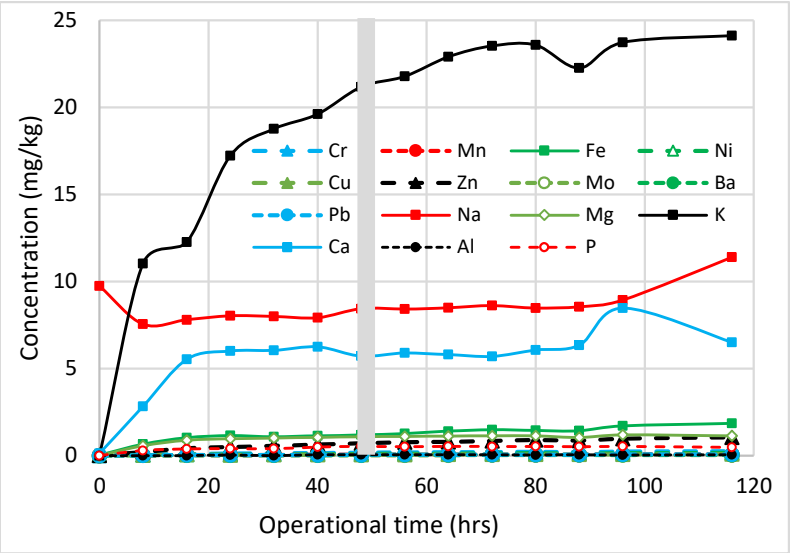

Figure 11: ICP-OES analysis of MEA samples (grey area indicates particulates collection period at the absorber inlet)

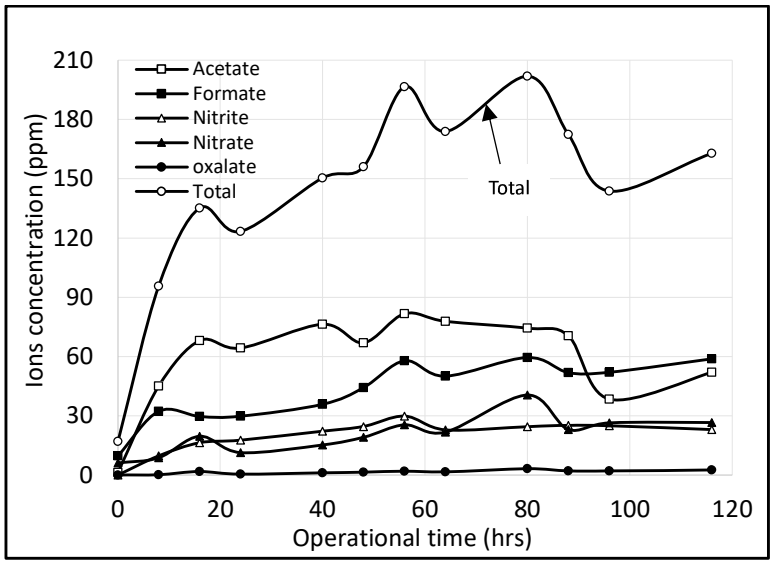

Figure 12: Anion concentrations in solvent samples